

CHARACTERISTICS OF Ph_3SnCl - doped PEO films.

3.1 Introduction

Different concentrations ($\text{Sn}/\text{EO}=0.015, 0.031, 0.063, 0.125$) of the PEO- Ph_3SnCl polymer electrolyte systems were prepared using the technique described in section 2.1.2. These electrolytes, however, showed low conductivities of the order of $10^{-7}\text{S}/\text{cm}$ at room temperature. For the efficient operation of solid state batteries at ambient temperatures, polymer electrolytes with conductivities of $10^{-5}\text{S}/\text{cm}$ or $10^{-3}\text{S}/\text{cm}$ are required [59]. Such conductivities could be approached in Ph_3SnCl -doped PEO (hereafter indicated as PEO- Ph_3SnCl) potentially by the co-addition of suitable plasticizers. In this study, two plasticizers, namely, ethylene carbonate (EC) and propylene carbonate (PC), were chosen. As described in section 2.1.2, blend electrolytes containing the dopant and the plasticizer were prepared. The best results were obtained using EC and PC together rather than individually. The composition that afforded the best conductivity of $1.1 \times 10^{-5} \text{ S}/\text{cm}$ was (PEO- Ph_3SnCl : EC: PC) 85:13:2. This electrolyte composition was hence used for the cell fabrication and study of discharge characteristics.

3.2 UV-Visible Spectral Analysis

UV-Visible spectra in acetonitrile of pure PEO film, PEO-doped Ph_3SnCl and PEO- Ph_3SnCl :EC:PC films are depicted in Figure 3.1. For purposes

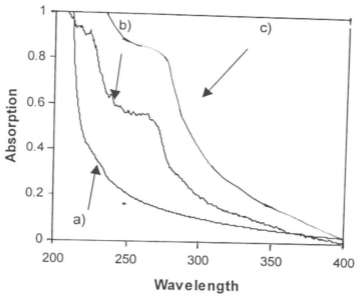


Figure 3.1: UV-Visible absorption spectrum for a) pure PEO film and b) PEO-Ph₃SnCl film c) PEO-Ph₃SnCl:EC:PC film.

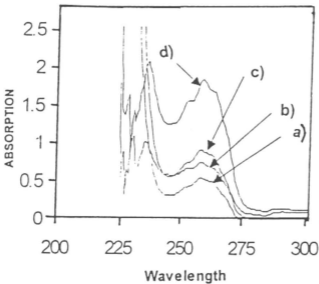


Figure 3.2 UV-Visible absorption spectra of two differing concentrations of Ph₃SnCl (a & b) and PEO - Ph₃SnCl:EC:PC (c & d) in acetonitrile.

of comparison, the spectra of pure Ph_3SnCl and of PEO- Ph_3SnCl : EC : PC mixed in the weight ratio (0.4:1:1:0.2) were recorded for two different substrate concentrations in acetonitrile as shown in Figure 3.2. It is seen that absorption spectra of the Ph_3SnCl and PEO - Ph_3SnCl :EC:PC are essentially unchanged at the two concentrations and both the samples reveal a characteristic band at 258nm. This band is ascribed to transitions within the energy levels of $(\text{Ph}_3\text{Sn})^+$ [60,61]. The peak at 231nm in PEO- Ph_3SnCl :EC:PC is that due to the plasticizer components, EC and PC.

As noted previously [62], PEO yields no peaks in the region 250nm to 800nm, whereas an absorption peak at 268nm is observed for PEO doped with Ph_3SnCl and PEO - Ph_3SnCl :EC:PC as shown in Fig 3.1. The shape of this peak is less well defined and appears shifted somewhat to longer wavelength relative to the case in pure Ph_3SnCl or PEO - Ph_3SnCl :EC:PC. While this cannot be attested as evidence for definitive interaction of Ph_3SnCl with the PEO, it does nevertheless suggest perturbation of the tin environment in the polymer. Thus UV-Visible spectroscopy confirms the presence of Ph_3SnCl in the PEO matrix.

3.3 IR - Spectral Analysis

The IR spectra of pure PEO, pure Ph_3SnCl and PEO doped with Ph_3SnCl are compared in Figures 3.3, 3.4, and 3.5 respectively. As can be seen, the salt free PEO polymer has distinct bands at 844 and 948 cm^{-1}

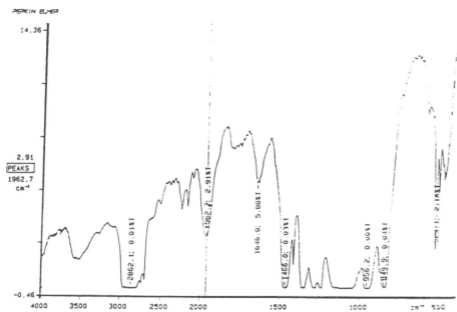
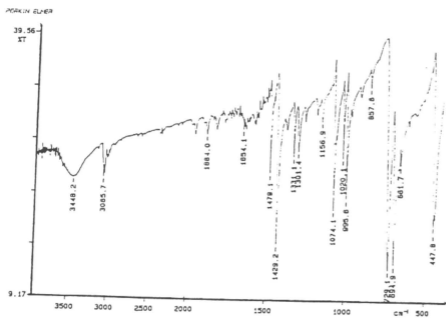


Figure 3.3: Infrared spectrum of pure PEO

Figure 3.4: Infrared spectrum of pure Ph₃SnCl

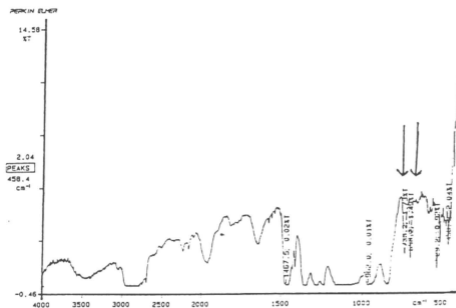


Figure 3.5: Infrared spectrum of PEO-Ph₃SnCl

which are assigned to CH₂ rocking modes in a gauche conformation [63] as well as a band 1153 cm⁻¹ which is assigned to anti symmetric C - O - C vibration [64]. Bands at (1235 cm⁻¹, 1282 cm⁻¹), (1358 cm⁻¹, 1417 cm⁻¹) and 1455cm⁻¹ are respectively ascribed to asymmetric CH₂ wagging [65] and asymmetric bending or deformation vibrations [66,67]. Other absorbance bands which occur in the region 2800cm⁻¹ – 3000cm⁻¹ are the result of the symmetric and asymmetric C-H stretching vibrations [68-70].

In the case of the PEO-Ph₃SnCl polymer complex, significant bands were observed at 698cm⁻¹ and 735cm⁻¹ as indicated by arrows in Figure3.5. These bands are shifted somewhat from the positions of the characteristic bands of pure Ph₃SnCl at 694cm⁻¹ and 729cm⁻¹, and may be indicative of complex formation between PEO and Ph₃SnCl.

3.4 DTA Analysis:

The results of DTA obtained for the samples of PEO and PEO doped with Ph_3SnCl at different concentrations ($\text{Sn}/\text{EO}=0.015, 0.031, 0.063, 0.125$) are shown respectively in Figures 3.6 and 3.7. The temperature range was from 30°C to 90°C ; the heating rate in all these experiments was 3°C per minute. As can be seen from the Figures, the melting point of the crystalline PEO did not deviate significantly from 68°C , but registered slight shifts dependent on the level of association of the dopant with the polymer.

Thus it is observed that the peak areas generally get smaller with increasing dopant concentrations although not in a proportionate manner. This indicates that with increasing dopant loading a reduction in crystallinity is suffered by the polymer, thereby increasing the amorphous fraction of the polymer.

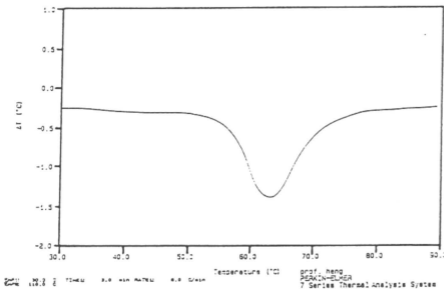


Figure 3.6: DTA plot for pure PEO.

3.4 DTA Analysis:

The results of DTA obtained for the samples of PEO and PEO doped with Ph_3SnCl at different concentrations ($\text{Sn}/\text{EO}=0.015, 0.031, 0.063, 0.125$) are shown respectively in Figures 3.6 and 3.7. The temperature range was from 30°C to 90°C ; the heating rate in all these experiments was 3°C per minute. As can be seen from the Figures, the melting point of the crystalline PEO did not deviate significantly from 68°C , but registered slight shifts dependent on the level of association of the dopant with the polymer.

Thus it is observed that the peak areas generally get smaller with increasing dopant concentrations although not in a proportionate manner. This indicates that with increasing dopant loading a reduction in crystallinity is suffered by the polymer, thereby increasing the amorphous fraction of the polymer.

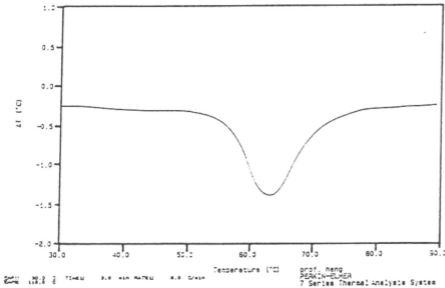


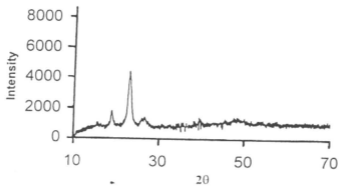
Figure 3.6: DTA plot for pure PEO.

of pure PEO, some additional diffraction peaks were also observed in the PEO- Ph_3SnCl systems at $2\theta = 13^\circ$ and $2\theta = 17^\circ$; these peaks are not observed in pure Ph_3SnCl used as the dopant material. From the XRD patterns of PEO- Ph_3SnCl systems, it can be inferred that at lower Ph_3SnCl content ($\text{Sn}/\text{EO} < 0.031$) most of the Ph_3SnCl dissolves within the crystalline phase of the PEO and the crystalline phase gets saturated as the concentration reaches $\text{Sn}/\text{EO} = 0.031$. However, above this limit ($\text{Sn}/\text{EO} > 0.031$) further addition of Ph_3SnCl gives rise to more amorphous films. Based on a consideration of physical and mechanical properties, films with concentration $\text{Sn}/\text{EO} = 0.031$ were considered to be the best for our studies. This is borne out from the conductivity studies discussed later in section 3.6.

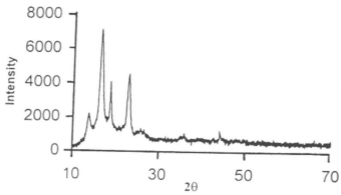
The XRD results suggest that part of the PEO remained as crystalline PEO and part of the PEO containing the dopant transformed into an amorphous phase thereby decreasing the overall degree of crystallinity of the polymer, in conformity with observations on other PEO-systems doped with inorganic salts [38,40]. This probably accounts for the higher conductivity values given by doped PEO samples relative to undoped PEO (*vide infra*).

The degree of crystallinity is related to the coherent length. For PEO - Ph_3SnCl complexes, the coherent length of each composition is evaluated from the diffraction peak at $2\theta = 24^\circ$. The longer the coherent

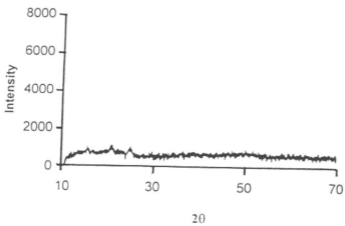
a) Pure PEO



b) Sn/EO = 0.015



c) Sn/EO = 0.031



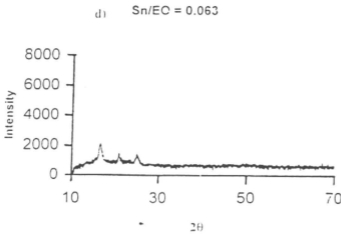
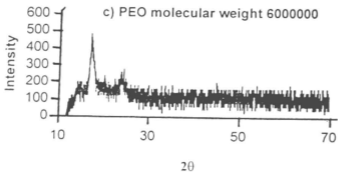
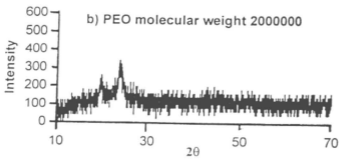
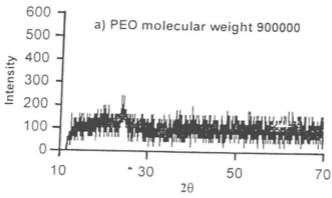


Figure 3.8: XRD patterns (a – d) for PEO - Ph_3SnCl system with differing Sn/EO ratios.

length, the more crystalline is the material. It is found that the coherent length decreases as the Sn/EO composition increases upto Sn/EO= 0.031 and at Sn/EO = 0.031 it becomes minimum. It is noted that the composition of 32:1 gives the shortest coherent length, meaning that it is the least crystalline in nature compared to other compositions. This may account for the highest electrical conductivity observed for this composition [71,72].

Also from the XRD patterns of samples prepared using different molecular weights of PEO, but with the same composition PEO - Ph_3SnCl : EC:PC (85:13:2), as shown in Figures 3.9(a - d) it can be inferred that the sample with the PEO molecular weight of 900000 is most amorphous compared to the others. This accounts for the highest electrical conductivity given by the sample, a result corroborated also by ac impedance results (sec.3.6).



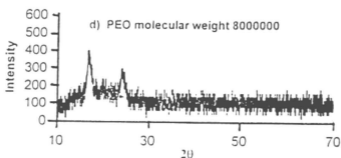


Figure 3.9: XRD patterns (a – d) for PEO – Ph_3SnCl system with different molecular weights of PEO.

3.6 Impedance Spectroscopy Analysis

It is necessary to know the electrical conductivity of the samples so that the sample with composition giving the highest electrical conductivity can be identified and used for the fabrication of electrochemical cells. Previous workers have measured the electrical conductivity at 1kHz frequency. It is realized that electrical conductivity measurements at 1 kHz may not give the true bulk conductivity [73]. Hence in this work we have used impedance spectroscopy to measure the electrical conductivity. With impedance spectroscopy, it is possible to differentiate processes occurring at the electrode – electrolyte junction and at the grain

boundaries with those occurring in the bulk.

3.6.1 Room Temperature Dependence of Electrical Conductivity

From the data of impedance spectroscopy, the Cole-Cole plot is constructed by plotting the imaginary impedance magnitude ($Z_i = Z \sin\theta$) against the real impedance magnitude ($Z_r = Z \cos\theta$). The Cole – Cole plot for different composition of PEO- Ph_3SnCl and PEO- Ph_3SnCl - EC: PC with different molecular weights of PEO are exhibited in Figures 3.10 (a - d) and 3.11 (a - d) from which the bulk resistance, R_b of each sample is determined and using the equation

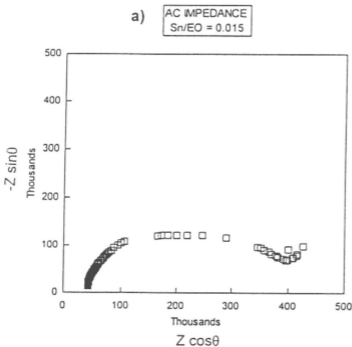
$$\sigma = L / R_b A \quad (3.1)$$

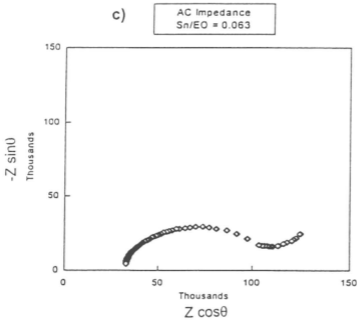
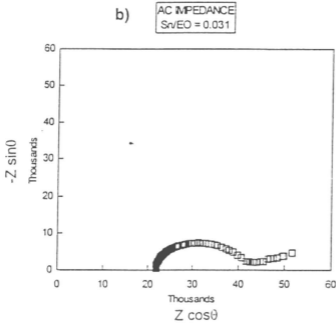
where σ is the electrical conductivity, L is the thickness of the sample, R_b is the bulk resistance and A is the electrode – electrolyte contact area. The electrical conductivity is then calculated and these values are tabulated in Table 3.1.

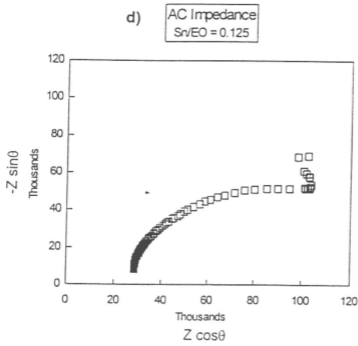
Table3.1: Ionic conductivity values calculated from the Cole-Cole plots of PEO- Ph_3SnCl .

Mole ratio of Sn/EO	Conductivity S/cm
0	4×10^{-9}
0.0078	3.5×10^{-8}
0.015	4.8×10^{-8}
0.031	3.6×10^{-7}
0.063	3×10^{-7}
0.125	1.4×10^{-7}

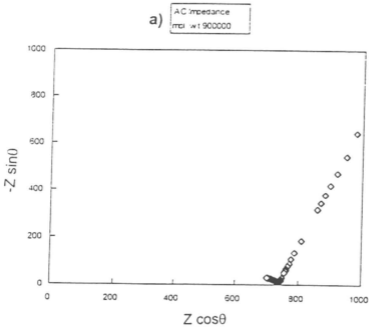
From table 3.1 it can be seen that the conductivity of the PEO – Ph_3SnCl systems vary with the Sn/EO ratio. With an increase in the Sn/EO ratio, the conductivity reaches a maximum of 3.6×10^{-7} S/Cm for Sn/EO = 0.031. It is well known that ionic conductivity occurs in the amorphous regions of a polymer [74]. This observation can therefore be attributed to the availability of conducting ions supplied by the dopant and to the increasing amorphous nature of the material as a result of polymer dopant interaction [75]. However, for higher salt concentrations Sn/EO > 0.031, the conductivity drops rapidly probably due to the salt segregation caused by the uncomplexed Ph_3SnCl . The trend is clearly shown in Figure 3.12 and such a behavior has been observed for many PEO based electrolyte systems [76-78].

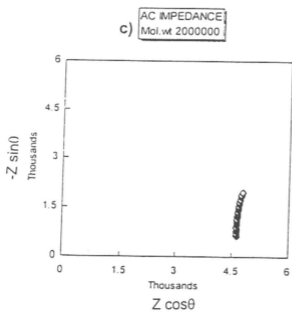
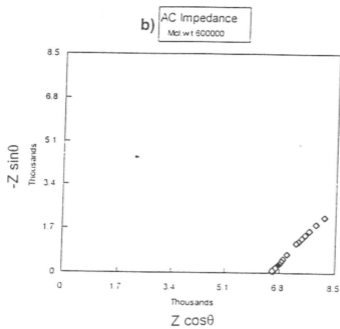






3.10: Cole – Cole plots (a - d) for different Sn/EO ratios in the PEO – Ph_3SnCl system.





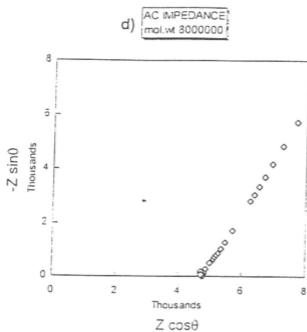


Figure 3.11: Cole – Cole plots (a - d) for the PEO – Ph_3SnCl system with different molecular weights for the PEO matrix.

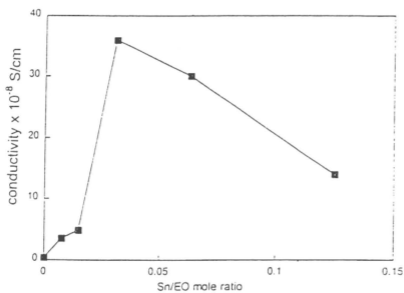


Figure 3.12: Compositional dependence of conductivity of PEO – Ph_3SnCl

Different molecular weights of PEO have been tried to find the effect of molecular weight on the conductivity and it was observed that PEO of molecular weight 900000 gives better conductivity as seen from the table 3.2.

Table 3.2: Conductivity data of PEO-Ph₃SnCl with different molecular weights of PEO

Molecular Weight	Conductivity(S/cm)
900000	1.1×10^{-5}
600000	1.2×10^{-6}
2000000	1.59×10^{-6}
8000000	1.57×10^{-6}

As these PEO-Ph₃SnCl polymer electrolytes cannot be used as electrolytes for all solid state batteries at ambient temperature for the reasons already discussed in section 3.1. In order to develop these polymer electrolytes to work at ambient temperature, two plasticizers (EC & PC) were added to the polymer electrolyte in a fixed ratio as given in section 2.1.2. In these electrolytes the solid polymer matrix provides good dimensional stability to the electrolyte while the high permittivity of ethylene carbonate and propylene carbonate enable extensive dissociation of the Ph₃SnCl. Also the low viscosity of EC and PC provides an ionic environment that facilitates high ionic mobility. Hence the best conducting sample with conductivity 1.1×10^{-5} S/cm was obtained for the composition (PEO-Ph₃SnCl:EC:PC) 85:13:2 and their values for other compositions were tabulated in table 3.3.

Table 3.3: Conductivity values of different samples of PEO - Ph₃SnCl: EC:PC

Sample composition Wt %	Electrical conductivity (S/cm)
85:13:2	1.1×10^{-5}
85:10:5	7.4×10^{-6}
85:8:7	3.6×10^{-6}
85:7.5:7.5	2.4×10^{-6}

3.6.2 Temperature Dependence of Electrical Conductivity

The temperature dependence of the electrical conductivity of PEO- Ph₃SnCl systems indicates an activated process. Thus the conductivity increases with increasing temperature [79] and Arrhenius behavior provides a good representation of the data in Table 3.4. The σ - T relationship is displayed in Figure 3.13. According to the data and from the graph it was observed that the system obeys Arrhenius behavior within the temperature 30°C to 70°C. Table 3.5 shows the Sn/EO mole ratio and activation energy values obtained from the $\ln \sigma T$ versus $10^3/T$ plots of Figure 3.13.

Table 3.4: Data for the generation of ($\ln(\sigma T)$ Vs $1/T$) plots for PEO – Ph₃SnCl systems.

$10^3/T$	$\ln(\sigma T)$ values for different compositions of Sn/EO					
(K ⁻¹)	0	0.0078	0.015	0.031	0.063	0.125
3.3	-13.62	-11.45	-11.14	-9.12	-9.3	-10.06
3.2	-13.22	-11.09	-10.82	-8.83	-8.96	-9.67
3.1	-12.80	-10.73	-10.5	-8.54	-8.62	-9.28
3.05	-12.60	-10.55	-10.34	-8.4	-8.45	-9.19
3.0	-12.41	-10.41	-10.17	-8.25	-8.28	-8.89
2.95	-12.20	-10.23	-10.01	-8.11	-8.11	-8.7
2.9	-11.98	-10.05	-9.85	-7.96	-7.94	-8.5
2.8	-10.58	-8.69	-7.54	-6.67	-6.1	-6.01
2.7	-9.82	-7.33	-7.23	-5.38	-5.26	-5.72

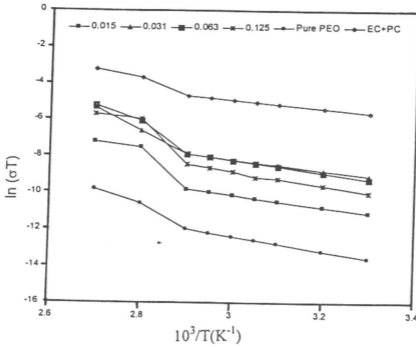


Figure 3.13: Arrhenius plots for the PEO- Ph_3SnCl system of varying compositions.

Table 3.5: Activation energy values, E_A , for PEO - Ph_3SnCl .

Mole ratio of Sn/Eo	Gradient ($-E_A/k$)	Activation energy(eV)
0	4000	0.34
0.0078	3600	0.31
0.015	3200	0.27
0.031	2900	0.25
0.063	3400	0.29
0.125	3900	0.33
PEO- Ph_3SnCl :EC :PC (85:13:2)	2400	0.21

According to the data and from the graph it was observed that the system obeys Arrhenius behavior within the temperature 30°C to 70°C . Table 3.5

shows the Sn/EO mole ratio and activation energy values obtained from the $\ln(\sigma T)$ versus $10^3/T$ plots of Figure 3.13. The E_A values obtained in this study compare favourably with literature values [74,80]. The increase in conductivity is attributed to the decrease in E_A while the decrease in conductivity beyond the Sn/EO = 0.031 ratio is attributed to the ions needing much more energy to begin motion. Such ionic conductivity activation energies have been reported for Li^+ conduction in reference [81] and supported also by NMR data [82].

Since conductivity is related to the number of carrier ions as well as their mobility, it can be concluded that the conductivity is influenced by many factors such as incorporated salt species, degree of crystallinity and morphological structure of polymer – salt complexes. Therefore to have a better understanding of and to seek further evidence for what has been stated above, it is necessary to carry out XRD and SEM.

3.7 SEM – EDAX Analysis

Scanning electron microscopy (SEM) was carried out to study the surface structure and morphology of the doped PEO. SEM photographs of films of pure PEO and PEO- Ph_3SnCl : EC:PC (of composition 85:13:2 as previously described) are depicted in Figures 3.14 and 3.15 respectively.

The SEM micrograph for pure PEO shows a spherulitic morphology

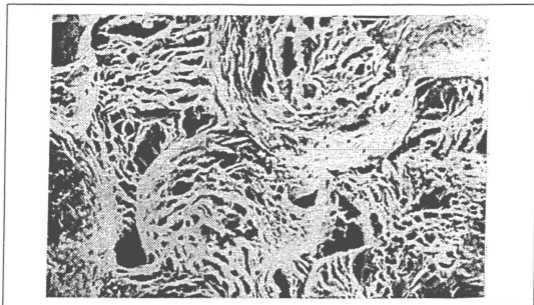


Figure 3.14: SEM micrograph for Pure PEO

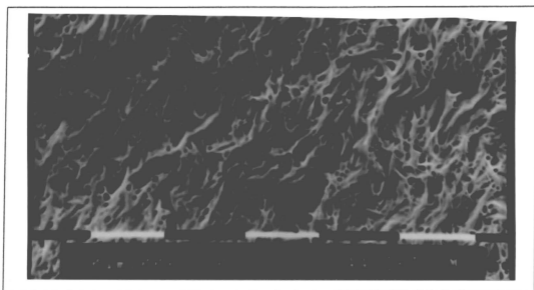


Figure 3.15: SEM micrograph for PEO-Ph₃SnCl: EC: PC

which is absent in the doped polymer. The spherulites represent the crystalline regions of the polymer [83-86], whose disappearance upon the addition of Ph₃SnCl and EC/PC suggests that the doped polymer is

essentially amorphous. This feature is also corroborated by the XRD patterns elaborated in section 3.5 (see Figure 3.8a and Figure 3.9 a).

Figure 3.16 shows the EDAX picture obtained upon analysing a sample of PEO- Ph_3SnCl (32:1) film. The peaks to Sn and Cl are clearly in evidence and attest unequivocally to the presence of Ph_3SnCl dopant in the polymer matrix.

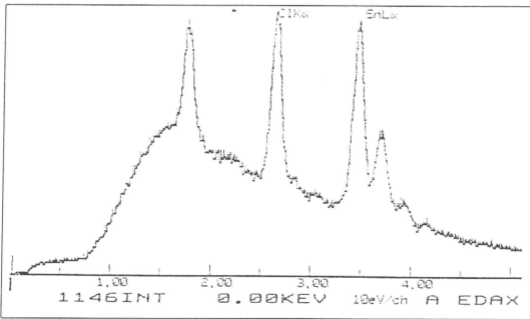


Figure 3.16: EDAX data for PEO- Ph_3SnCl

3.8 Possible Conduction Mechanism

Poly(ethylene oxide) PEO, being highly stereoregular has the following structure as shown in Figure 3.17a . The thick dark line in the figure represents the polymer backbone, the big open circles attached to it are the oxygens of the PEO and the small dark circles represent the cationic species. In the present context, the cationic species probably represent

$(\text{Ph}_3\text{Sn})^+$.

The well-known acceptor character properties of tin combined with its proclivity to bind to hard bases favours strong interaction with the oxygen atoms of PEO. Electrical neutrality is preserved by the chloride ions whose close proximity to the tin may thus be not critical as would otherwise be the case in an intimate ion-pair situation. The ionic transport in the doped polymer at the polymer glass transition temperature ($T_g \cong 60^\circ\text{C}$) may be interpreted on the basis of a hopping mechanism between the polymer chains as shown in Figures 3.17 (b & c). For temperatures above the T_g value, the polymer behaves as a highly viscous liquid (elastomer) and this in turn imparts increased mobility to the ions on account of the disordered movements of the chain as shown in Figures 3.17 (d & e).

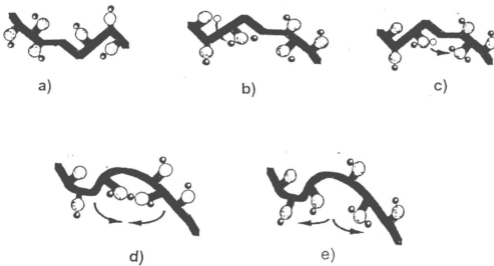


Figure 3.17: Possible conduction mechanism in PEO - Ph_3SnCl system.

3.9 Electrochemical Cell Characterization

Films of PEO- Ph_3SnCl : EC: PC with composition 85:13:2 which showed the highest electrical conductivity in tests using impedance spectroscopy were used as the electrolyte component in the electrochemical cell fabrication. The anode consisted of Sn metal foil while the cathode consisted of intercalated composite cathodes of MnO_2 and I_2 deposited as a film on copper mesh as described in section 2.1.3. The anode, electrolyte and the cathode were then clamped between two glass plates and then connected via the electrodes to a computer-controlled galvanostat (BAS LG - 50) for characterization and discharge characteristics.

Figure 3.18 shows the discharge characteristics for the fabricated cells. The cells were discharged at $10\mu\text{A}$. It is found that the voltage of the cell drops at the beginning of the discharge and as the discharge proceeds the voltage seems to be quite stable for many minutes in the plateau region before it decreases again. This may account for the build up of the internal resistance in the cell at the beginning of the discharge due to interfacial resistance between the anode-electrolyte and cathode-electrolyte interface. After several hours of discharge, this interfacial resistance is reduced probably due to a better contact formed between the electrode and the electrolyte and results in constant voltage in the plateau region. Prior to discharge, the open circuit voltage (OCV) of the

two fabricated cells were measured; the values are given in Table 3.6

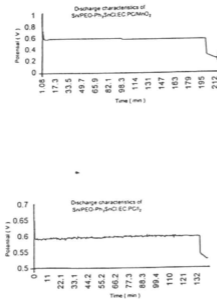


Figure 3.18: Discharge curves for the fabricated electrochemical cells using different cathode materials.

Table 3.6: Open circuit voltage for the fabricated cells.

SAMPLE COMPOSITION	OCV
Sn/PEO-Ph ₃ SnCl:EC:PC/MnO ₂	0.8 V
Sn/PEO-Ph ₃ SnCl:EC:PC/I ₂	0.65V

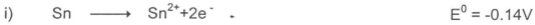
Discharge curves such as depicted in Figure 3.18 are useful, in that they allow estimation of the cell capacity, based on the relation, Cell Capacity = discharge current associated with the plateau region x Time span of the plateau. The cell capacity thus obtained are tabulated in Table 3.7. These values are found to be very low when compared with other current commercial systems like Ni-Cd cell which has 300 mA-h of cell capacity. This may be due to the low ionic conductivity of the sample.

Table 3.7: Cell capacity of fabricated cells

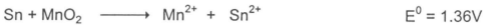
SAMPLE COMPOSITION	CELL CAPACITY(mA-h)
Sn/PEO-Ph ₃ SnCl:EC:PC/MnO ₂	0.0325
Sn/PEO-Ph ₃ SnCl:EC:PC/I ₂	0.0225

The possible electrode reactions occurring in the cell Sn/PEO-Ph₃SnCl:EC:PC/MnO₂ can be represented as

a) Oxidation at the Sn anode:



a) Reduction at the cathode.



From these cell reactions the theoretical OCV of the above cell is 1.36V.

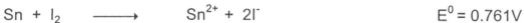
The experimentally obtained OCV is about 60% of the theoretical value.

In the cell Sn/PEO – Ph₃SnCl - EC - PC/I₂ the OCV obtained is 0.65V. The possible cell reactions occurring in this cell can be

a) Oxidation at anode: -



a) Reduction at cathode:-



From these half-cell reactions the theoretical OCV is 0.761V and the experimentally obtained OCV is about 80% of the theoretical value.